SUPPLEMENTARY INFORMATION

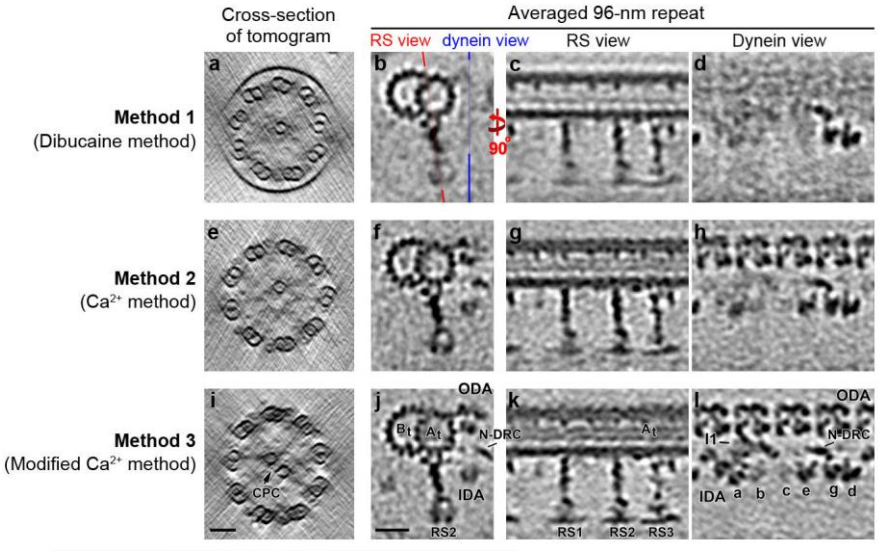

Supplementary Figure 1. Improved structural preservation by optimization of the cilia preparation method for cryo-ET. (**a**-**d**) Method 1: Normal human ciliary axonemes were isolated by the dibucaine method[1,2]. A 100-nm-thick cross-sectional tomographic slice (**a**) shows an individual 3D-reconstructed axoneme. A 5-nm-thick cross-sectional tomographic slice (**b**) and two 10-nm-thick longitudinal tomographic slices (**c** and **d**) show the averaged normal human 96-nm axonemal repeat prepared with Method 1. In particular, the dynein view (**d**) shows the artificial extraction of almost all ODAs and several IDAs. (**e**-**h**) Method 2: Normal human ciliary axonemes were isolated following a previously published and widely used protocol[3-5]. In particular, the dynein view (**h**) shows the artificial extraction of several IDAs. Note that the cilia membranes were removed by the detergent included in this method (**e**). (**i**-**l**) Method 3: Normal human ciliary axonemes were isolated by our modified Ca^{2+} method (see Methods for details). Most axonemal structures appear well preserved in the subtomogram average, including most IDAs (dyneins a-g), making method 3 the clear choice for the structural study of human motile cilia by cryo-ET. Scale bars: (**a**, **e**, and **i**) 50 nm, (**b**-**d**, **f**-**h**, and **j**-**l**) 20 nm.

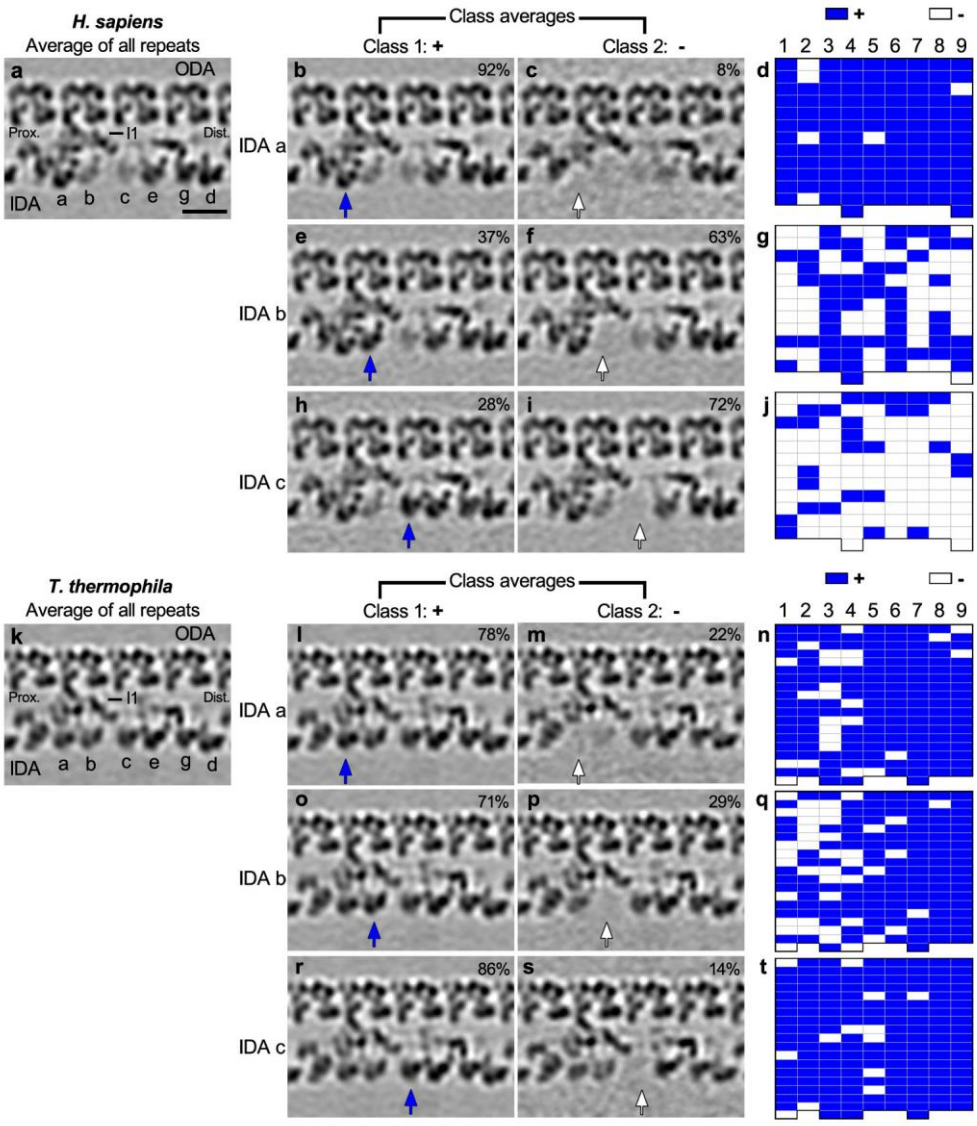

Supplementary Figure 2. The classification analysis of axonemal repeats from normal human cilia (a-j) and wild-type *Tetrahymena* cilia (k-t) shows that some IDAs are prone to extraction from axonemal repeats during the isolation procedure for axonemes. The right column shows charts that represent the distribution pattern of axonemal repeats with (blue boxes) and without (white boxes) a specific IDA isoform (IDA a, b, or c) in one representative normal human (**d**, **g**, **j**) or wild-type *Tetrahymena* (**n**, **q**, **t**) axoneme; the nine DMTs are numbered 1-9. All other images show longitudinal tomographic slice of subtomogram average of axonemal repeats either of normal human (top half) or of wild-type *Tetrahymena* (bottom half) cilia. Subtomogram averages that include all 96-nm repeats show that the densities of IDAs b and c appear weaker than other IDAs in normal human axonemes (**a**) and slightly weaker in wild-type *Tetrahymena* axonemes (**k**). (**b-j** and **l-t**) Analyzing this in more detail, we performed a classification analysis focusing on different IDA isoforms. This analysis revealed that in both normal human and wild-type *Tetrahymena* cilia the axonemal repeats with (blue arrow) or without (white arrow) IDA a, b or c are randomly distributed among the nine DMTs. Scale bar: (**a-c**, **e**, **f**, **h**, **i**, **k-m**, **o**, **p**, **r**, and **s**) 20 nm.

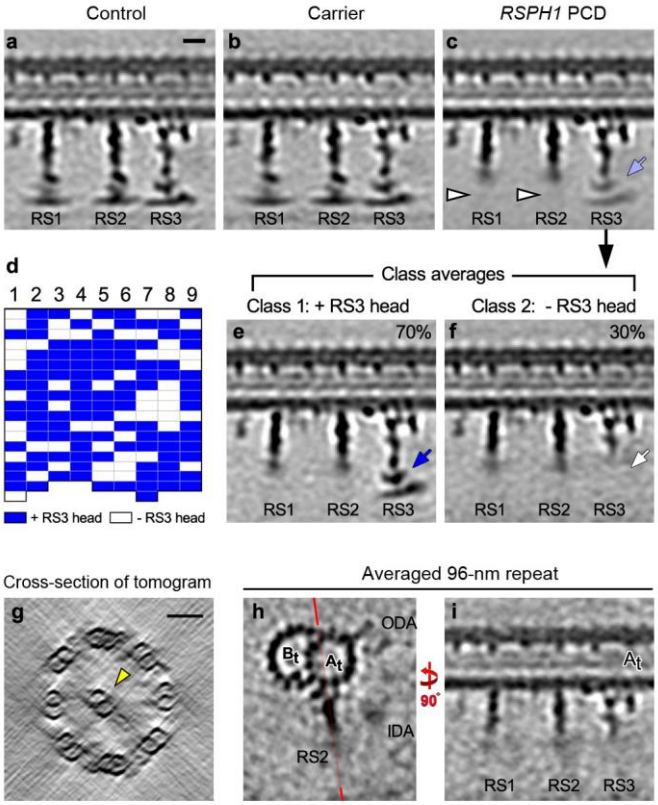

Supplementary Figure 3. Cryo-ET reveals structural defects in the radial spokes of human *RSPH1* PCD cilia. (**a-c**) 10-nm-thick longitudinal tomographic slices show the averaged 96-nm repeat after averaging multiple axonemes from normal control (**a**), carrier (**b**), and *RSPH1* PCD samples (**c**). Arrowheads highlight the primary defects in *RSPH1* PCD cilia: the distal regions, including the RS heads of RS1 and RS2 are missing. Note that the density of the spoke head of RS3 (light blue arrow) appears weaker than other axonemal structures, such as the stem densities of all RSs. (**d-f**) A classification analysis of the subtomogram averages reveals that the RS3 head is missing in some axonemal repeats. The distribution pattern of axonemal repeats with (blue boxes) and without (white boxes) the RS3 head in a representative *RSPH1* PCD human ciliary axoneme reveals that the classes are randomly distributed among the nine DMTs (**d**). Dark blue (**e**) and white (**f**) arrows indicate the presence and absence of RS3 head in the class averages of axonemal repeats, respectively. (**g-i**) A DMT translocated to the center of an (8+1)+0 axoneme from an *RSPH1* PCD patient also shows the RS head defects. A 100-nm-thick cross-sectional tomographic slice (**g**) shows an (8+1)+0 axoneme. A 5-nm-thick cross-sectional tomographic slice (**h**) and a 10-nm-thick longitudinal tomographic slice (**i**) show the averaged 96-nm axonemal repeat from the centrally located DMT. Note that all RS heads, including RS3, seem to be missing from the averaged repeat of the translocated DMT, indicating that they are lost in most or all axonemal repeats. The orientation of the slice (**i**) is indicated in (**h**). Scale bars: (**a-c**, **e**, **f**, **h**, **i**) 10 nm, (**g**) 50 nm.

Supplementary Table 1. Samples used in this study

Organism	Genotype	Number of tomograms	Averaged repeats	Resolution (nm)
H. sapiens	Normal control (i.e., non-PCD; non-cystic fibrosis)	12	850	3.4
	Heterozygote carrier *RSPH1*$^{+/-}$	5	650	3.4
	PCD patient *RSPH1*$^{-/-}$	20	1020	3.4
S. purpuratus *	Wild type	9	1100	3.4
T. thermophila (CU428)	Wild type	12	760	3.3
C. reinhardtii * (*pf2-4::PF2-GFP* †)	Pseudo wild type	5	720	3.1

* Some of the tomograms from these strains were published previously[6,7].

† Strain was provided by Raqual Bower and Mary E. Porter (University of Minnesota) and generated by rescuing the N-DRC-defective *pf2* mutant strain with a GFP-tagged wild-type *PF2* gene[8]. This strain is structurally and phenotypically indistinguishable from the wild type[7].

Supplementary References

1. Pigino, G. *et al.* Cryoelectron tomography of radial spokes in cilia and flagella. *J. Cell Biol.* **195,** 673-687 (2011).
2. Witman, G. B. Isolation of *Chlamydomonas* flagella and flagellar axonemes. *Methods Enzymol.* **134**, 280-290 (1986).
3. Hastie, A. T. *et al.* Isolation of cilia from porcine tracheal epithelium and extraction of dynein arms. *Cell Motil. Cytoskeleton.* **6,** 25-34 (1986).
4. Ostrowski, L. E. *et al.* A proteomic analysis of human cilia: identification of novel components. *Mol. Cell Proteomics* **1,** 451-465 (2002).
5. Kultgen, P. L., Byrd, S. K., Ostrowski, L. E. & Milgram, S. L. Characterization of an A-kinase anchoring protein in human ciliary axonemes. *Mol. Biol. Cell* **13,** 4156-4166 (2002).
6. Lin, J., Okada, K., Raytchev, M., Smith, M. C. & Nicastro, D. Structural mechanism of the dynein power stroke. *Nat. Cell Biol*. **16,** 479-485 (2014).
7. Heuser, T., Raytchev, M., Krell, J., Porter, M. E. & Nicastro, D. The dynein regulatory complex is the nexin link and a major regulatory node in cilia and flagella. *J. Cell Biol.* **187,** 921-933 (2009).
8. Bower, R. *et al*. The N-DRC forms a conserved biochemical complex that maintains outer doublet alignment and limits microtubule sliding in motile axonemes. *Mol. Biol. Cell* **24,** 1134-1152 (2013).